Stationary and dynamical aspects of two-magnon states in disordered ferromagnetic chains

E. M. Nascimento, F. A. B. F. de Moura, and M. L. Lyra
Departamento de Física, Universidade Federal de Alagoas, 57072-970 Maceió, AL, Brazil
(Received 15 July 2005; revised manuscript received 21 October 2005; published 14 December 2005)

We study the nature of collective two-spin excitations in disordered $S=1/2$ ferromagnetic chains. Using a direct diagonalization scheme, we characterize the two-magnon eigenstates by computing their spacial extent, two-point correlation and the average distance between the excited spins within the allowed energy band. We found that, due to the effective excitation interaction imposed by the exclusion rule, the low-energy two-magnon states display strong spin-spin correlations as compared to the more localized high-energy states. We further solve the time-dependent Schroedinger equation to follow the time evolution of an initially localized two-magnon state. We show that the effective one-magnon wave packet develops power-law tails with distinct exponents for the left and right tails, with the distribution function of the spin-spin distance decaying as $P(d) \propto 1/d$. We show that the average distance between the two excited spins evolves in time diffusively, while the wave-packet dispersion evolves superdiffusively.

DOI: 10.1103/PhysRevB.72.224420 PACS number(s): 75.10.Jm, 71.23.An, 75.40.Gb

I. INTRODUCTION

The nature of collective single-spin excitations in random ferromagnetic systems has a close relationship with the one-electron eigenstates in tight-binding models of noninteracting electrons in random media.[1–9] In a three-dimensional lattice the presence of weak disorder promotes the localization of the high-energy spin-waves. The low-energy states with long wavelength remain extended, although acquiring a finite coherence length. A mobility edge separates the high-energy localized from the low-energy extended states. The position of the mobility edge continuously decreases as the disorder, strength is enhanced. In the regime of strong disorder, all magnon states become exponentially localized.

At low dimensions, specially in one-dimensional disordered ferromagnetic chains, the finite energy states are exponentially localized for any degree of disorder, resembling the prediction of the scaling theory for the Anderson localization transition.[3] However, because the low-energy states have a long wavelength, they exhibit a typical localization length that diverges as one approaches to the bottom of the band. This feature results in quite particular features related to the transport of magnetic excitations in low-dimensional random ferromagnets that are not shared by the electronic counterpart. For example, an initially localized spin excitation may exhibit a superdiffusive spread in the presence of disorder in contrast to the random oscillations over a finite segment displayed by an electron wave packet.[7,8]

The interplay between disorder and electron-electron interaction has been the subject of great interest due to their competitive role.[10–20] It has been shown that on-site Hubbard-like interactions weakens the Anderson localization induced by disorder. As a result, an enhanced propagation of an interacting electron pair can be obtained over distances larger than the single-particle localization length, as indeed predicted in disordered mesoscopic rings threaded by magnetic flux.[12] However, the interaction becomes effective only for those localized states that are in positions close to each other. Therefore, the Anderson localization weakening observed in mesoscopic rings vanishes for an infinite chain, following the vanishing of the fraction of overlapping localized electron states.[21]

Because of the long localization length of the low-energy magnon states, the spin-spin interaction effect in random $S=1/2$ ferromagnetic chains is expected to influence the magnetic transport even in the infinite chain limit. Spin-wave interactions have attracted a long-standing interest since the pioneering work of Dyson,[22] and the nature of multimagnon excitations has been studied by different techniques.[23–27] Recently, it has been pointed out that understanding the interplay between interaction and disorder is a prerequisite for building a quantum computer.[28] Localized two-magnon states were shown to form around defects in inhomogeneous ferromagnetic systems.[29,30]

In order to further explore the above phenomenology, we are going to employ a detailed analysis of the nature of the two-magnon excitations in finite-disordered chains. As a $S=1/2$ spin only allows for a single excitation (i.e., two spin excitations can never occupy the same site), the effective spin-spin interaction is closely related to an infinite strength Hubbard repulsion. Some relevant properties of the stationary two-magnon states will be computed using a direct numerical diagonalization algorithm on finite chains, together with a finite-size scaling analysis. The localization length will be characterized by the participation number and spacial extent of the two-magnon states. The spin-spin correlation will also be reported to reveal the distinct finite-size effects over low and high energy states. Finally, we will solve the time-dependent Schroedinger equation to follow the time evolution of an initially localized two-magnon state. The diffusive character of the average spin-spin distance and the superdiffusive wave-packet spread will be reported and related to the asymptotic form the two-magnon wave packet.

II. MODEL AND FORMALISM

We will consider finite disordered chains of $S=1/2$ spins coupled via a first-neighbors isotropic Heisenberg exchange interaction, whose Hamiltonian can be written as

$$H = -\sum_n J_{n,n+1} \vec{S}_n \cdot \vec{S}_{n+1}, \quad (1)$$

where the couplings $J_{n,n+1}$ are uncorrelated random ferromagnetic couplings, which can assume the values J_1 and J_2 with equal probability. In what follows we will work in units of $J_1=1$. The ground state for a ferromagnetic chain consists of a perfectly ordered chain with all spins aligned on the same direction. We will refer to the ground state as the vacuum state $|0\rangle$ in what concerns to the presence of magnetic excitations. One-magnon states are the Hamiltonian eigenstates on the subspace generated by all single-flip states $|\phi_n\rangle = S_n^-|0\rangle$. In the presence of disorder, the one-magnon states are spatially localized, with the characteristic localization length diverging as one approaches the bottom of the excitation energy band. Here we will explore the nature of the Hamiltonian eigenstates on the subspace generated by all two flip states. The bases for this subspace can be represented by

$$|\Phi_{n_1,n_2}\rangle = S_{n_1}^- S_{n_2}^-|0\rangle, \quad (2)$$

where $|\phi_{n_1,n_2}\rangle$ is the state with spin flips located at sites n_1 and n_2. In the absence of disorder, most of the two-magnon eigenstates on a chain with N spins are unbounded and their energy spectrum ranges from $0<E<4J$. However, N out of the $N(N-1)/2$ possible two-magnon states are bounded states and distributed over an energy range $0<E<2J$. In the presence of disorder, there is no clear distinction between bounded and unbounded states. In order to characterize the nature of the two-magnon eigenstates, we shall solve the time-independent Schroedinger equation to obtain the coefficients ϕ_{n_1,n_2} in the expansion over the two-flip bases $|\Phi\rangle = \Sigma \phi_{n_1,n_2}|\phi_{n_1,n_2}\rangle$. The coefficients obey the following recursion relation:

$$\begin{aligned} 2\epsilon\phi_{n_1,n_2} = {} & (J_{n_1-1,n_1} + J_{n_1,n_1+1} + J_{n_2-1,n_2} + J_{n_2,n_2+1})\phi_{n_1,n_2} \\ & - J_{n_1,n_1+1}\phi_{n_1+1,n_2} - J_{n_2,n_2+1}\phi_{n_1,n_2+1} - J_{n_1,n_1-1}\phi_{n_1-1,n_2} \\ & - J_{n_2-1,n_2}\phi_{n_1,n_2-1}, \end{aligned} \quad (3)$$

for n_1 and n_2 not being neighboring sites. The eigenstate coefficient for flips at neighboring sites follows a simpler recursive relation in the form:

$$\begin{aligned} 2\epsilon\phi_{n,n+1} = {} & (J_{n-1,n} + J_{n+1,n+2})\phi_{n,n+1} - J_{n+1,n+2}\phi_{n,n+2} \\ & - J_{n-1,n}\phi_{n-1,n+1}. \end{aligned} \quad (4)$$

The above set of $N(N-1)/2$ equations provides the coefficients of all two-magnon eigenstates. As the numerical algorithm requires the diagonalization of $M \times M$ matrices, with $M=N(N-1)/2$, we are restricted to compute the two-magnon states on relatively small chains. In order to infer about the limit of infinite chains, we will employ a finite-size scaling analysis. In Sec. III, we will show results derived from the stationary states on chains with $N=21$, 41, and 81 spins. Distinct realizations of the distribution of exchange couplings will be accounted to perform a configurational average over the disorder, namely, 8000 realizations for the smallest chain size and 500 realizations for the largest one.

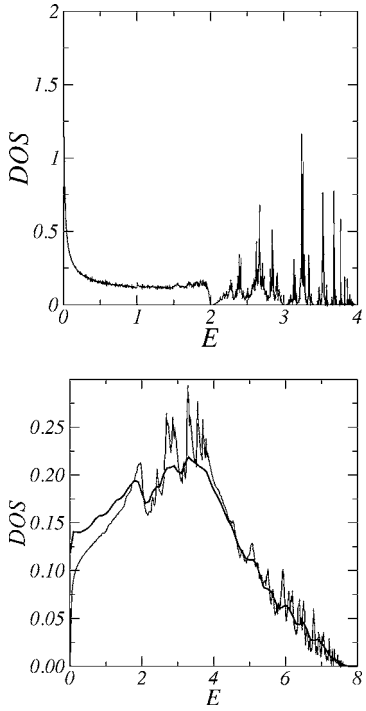

FIG. 1. (a) One-magnon density of states obtained from the negative eigenvalue theorem applied to $N=10^4$ chains with $J_2/J_1=2$. The two-band structure resembles the DOS of an alternate binary ferromagnetic chain. (b) Two-magnon density of states from exact diagonalization of chains with $N=90$ sites (thick line). It has a single-band structure. The thin line is a convolution of the one-magnon DOS, which represents the large chain limit of the two-magnon DOS. The deeps are related to small gaps in the one-magnon DOS.

At first, we report in Fig. 1 the density of one- and two-magnon states. The one-magnon density of states (DOS), obtained using the negative eigenvalue theorem applied to a chain with 10^4 spins, has two main energy bands (which resembles the DOS of an alternate binary ferromagnetic chain). Disorder introduces stronger DOS fluctuations at the high-energy band. On the other side, the two-magnon DOS was computed from exact diagonalization of chains with 90 sites. It exhibits a single-band structure. Such density of states contains finite size corrections. Its thermodynamic form can be fairly well estimated [thin line in Fig. 1(b)] through a convolution of the one-magnon DOS, once two-magnon interaction may be disregarded in the limit of very long chains. Note that the two-magnon DOS develops deeps at energies around $E=2$ and $E=3$, which are related to a vanishing one-magnon DOS around these energies.

III. THE NATURE OF TWO-MAGNON EIGENSTATES

To characterize the nature of the two-magnon stationary states, we start by computing the average distance d of the two flipped spins. For a given eigenstate, it is defined as

$$d = \sum_{n_1<n_2} (n_2 - n_1)|\phi_{n_1,n_2}|^2. \quad (5)$$

In this section, we will present results for the particular case of $J_2/J_1=2$. All quantities for a given configuration of disor-

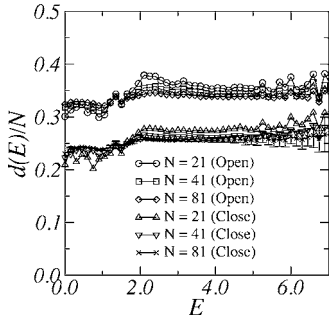

FIG. 2. Average distance between the flipped spins vs energy for finite chains with open and closed boundary conditions. The average distance is roughly constant with distinct corrections to scaling at low and high energies. The crossing signals the edge of the reminiscent bound states band. The representative error bars shown account for fluctuations due to distinct disorder configurations. The larger values at the upper-band edge reflects the vanishing of the density of states.

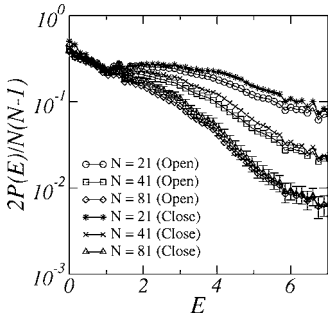

FIG. 3. Normalized average participation number (P/M) of two-magnon states vs energy in open and closed disordered ferromagnetic chains $[M=N(N-1)/2]$. The collapse of data for the low-lying states indicates that the asymptotic localization length in the thermodynamic regime is much larger than the chain sizes considered. Error bars account for fluctuations over disorder configurations.

der were computed as an average over the eigenstates with energies in a small interval around E. We further performed an average over disorder. The reported error bars account for fluctuations due to random exchange configurations. For the sake of clarity, we will include in the figures just the error bars corresponding to a single representative case. In Fig. 2, we plot the average distance $d(E)$, which consists of the average distance between the flipped spins, taking into account all eigenstates with energy in a small interval around E. For a very large chain, one expects that the average distance between the flipped spins can be estimated, assuming their positions as random. This feature just reflects the fact that localized one-magnon states with a particular energy can be at arbitrary distances. In chains with open boundary conditions, the average distance should then approach $\langle d\rangle_o = N/3$, while for chains with periodic boundary conditions it shall reduce to $\langle d\rangle_p = N/4$. Figure 2 exhibits the above trends, but finite-size corrections are in distinct directions for high- and low-energy two-magnon states. The finite-size correction toward larger distances observed for the high-energy states in finite chains is mainly due to the fact that double occupancy is not allowed. On the other hand, the correction to smaller distances of the low-energy states has a contribution reminiscent from the low-energy two-magnon bound states. The crossing around $E=2$ signals the edge of the bound states band.

In order to study the spacial distribution of the two-magnon states, we computed the participation number of each eigenstate defined as

$$P = \frac{1}{\sum_{n_1<n_2} |\phi_{n_1,n_2}|^4}. \tag{6}$$

In Fig. 3, we plot the normalized average participation number $P(E)$, taking into account all states within a small energy window around E. For extended two-magnon states, it shall scale as N^2 [actually the maximum participation number is $N(N-1)/2$ for a uniform state]. The states with localization length smaller than the chain size have size-independent participation numbers. Our results show that the high-energy states are well localized presenting a short localization length. The localization length is larger for the low-energy states. The collapse of data from distinct chain sizes for small excitation energies indicates that the localization length on an infinite chain is much larger than the chain sizes considered. To further characterize the spatial extension of the two-magnon states on disordered ferromagnetic chains, we computed the eigenstates spatial extent defined as

$$\xi = \sum_{n_1<n_2} |\phi_{n_1,n_2}|^2 \sqrt{(n_1 - \langle n_1\rangle)^2 + (n_2 - \langle n_2\rangle)^2}, \tag{7}$$

where

$$\langle n_i\rangle = \sum_{n_1<n_2} n_i |\phi_{n_1,n_2}|^2, \quad i = 1,2, \tag{8}$$

which gives a measure of the wave-function spread on the $n_1 \times n_2$ plane. The averaged spatial extent $\xi(E)$ of all two-magnon states in a small window around E is reported in Fig. 4. These results show that the high-energy two-magnon states have a relatively small spatial extent and that periodic

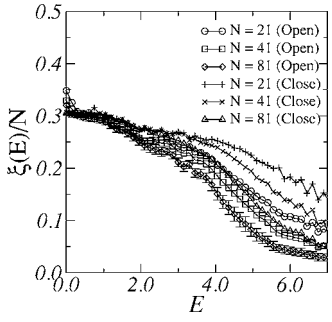

FIG. 4. Average normalized spacial extent $\xi(E)$ vs energy for two-magnon states of finite disordered ferromagnetic chains. The trends are similar to those exhibited by the participation number. Periodic boundary conditions implies in less localized states. At the bottom of the energy band $\xi(E\to 0)\simeq 0.3$. Error bars account for fluctuations over disorder configurations.

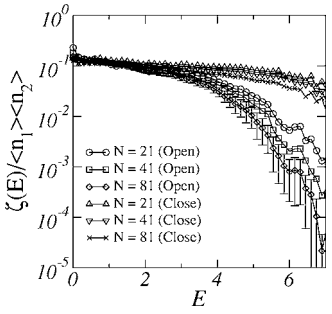

FIG. 5. Average relative correlation function of two-magnon eigenstates vs energy for finite disordered ferromagnetic chains. The correlation at low energies results from the strong effect caused by the constraint $n_1 < n_2$ on states with long localization lengths. Localized high-energy states are less correlated in open than in closed chains. Error bars account for fluctuations over disorder configurations.

boundaries implies in less localized states. This trend was also evidenced in the participation number results. The collapse of data at low energies reinforces the large spatial extent of the low-lying states with $\xi(E \to 0)/N \simeq 0.3$.

The effective interaction between the flipped spins in the two-magnon states can be numerically probed by computing the two-point correlation function of each eigenstate, written as

$$\zeta = \langle n_1 n_2 \rangle - \langle n_1 \rangle \langle n_2 \rangle, \tag{9}$$

where $\langle n_1 \rangle$ and $\langle n_2 \rangle$ are the average positions of the flipped spins given by (8) and

$$\langle n_1 n_2 \rangle = \sum_{n_1 < n_2} n_1 \cdot n_2 |\phi_{n_1,n_2}|^2. \tag{10}$$

The constraint of $n_2 > n_1$ promotes strong correlations between the flipped spins whenever the wave-function spatial extent is large, i.e., in low-energy two-magnon states. Assuming the two-magnon wave function to be uniformly distributed, although satisfying the above restriction, one can directly demonstrate that $\langle n_1 \rangle = N/3$, $\langle n_2 \rangle = 2N/3$, and $\langle n_1 n_2 \rangle = N^2/4$. This gives an estimate for the relative correlation function at low energies as being $\zeta / \langle n_1 \rangle \langle n_2 \rangle = 1/8$. In Fig. 5 we report the relative correlation function as obtained from finite chains, which corroborates the above estimate. The correlation $\zeta(E)$ was computed as the average correlation of all states with energy around E. As expected the high-energy states are weakly correlated because of the exponential localization of the two-magnon states, with the correlation dependence on the eigenstate energy being slower in closed than in open chains.

IV. TWO-MAGNON WAVE-PACKET DYNAMICS

The long localization length of the low-energy one-magnon states causes a superdiffusive spread of an initially localized wave packet.[7] Therefore, a similar diffusivelike dynamics is expected to take place associated with two-magnon excitations. In this section, we will investigate the time evolution of a wave packet initially composed of two flipped spins at a distance d_0. We numerically solve the time-dependent Schroedinger equation $i\hbar(d/dt)|\Phi(t)\rangle = H|\Phi(t)\rangle$ where H is the Hamiltonian (1) and $|\Phi(t)\rangle = \Sigma_{n_1<n_2} \phi_{n_1,n_2}(t) |\phi_{n_1,n_2}\rangle$. The time-dependent coefficients $\phi_{n_1,n_2}(t)$ obey a set of differential equations, derived from (4), for spin deviations at neighboring sites and from (3) for non-neighboring deviations, namely,

$$i\frac{d\phi_{n,n+1}(t)}{dt} = (J_{n-1,n} + J_{n+1,n+2})\phi_{n,n+1}(t) - J_{n+1,n+2}\phi_{n,n+2}(t) - J_{n-1,n}\phi_{n-1,n+1}(t) \tag{11}$$

and

$$i\frac{d\phi_{n_1,n_2}(t)}{dt} = (J_{n_1-1,n_1} + J_{n_1,n_1+1} + J_{n_2-1,n_2} + J_{n_2,n_2+1})\phi_{n_1,n_2} - J_{n_1,n_1+1}\phi_{n_1+1,n_2}(t) - J_{n_2,n_2+1}\phi_{n_1,n_2+1} - J_{n_1-1,n_1}\phi_{n_1-1,n_2} - J_{n_2-1,n_2}\phi_{n_1,n_2-1}, \tag{12}$$

$$n_2 > n_1 + 1,$$

where we used units of $\hbar = 1$. The above set of equations were numerically solved by using the fourth-order Runge-Kutta method on open chains up to $N = 800$ sites.

The destructive interference between the wave reflected at the chain boundaries and the outgoing wave leads to a non-uniform envelope of the asymptotic wave packet after a very long time evolution. A power-law asymptotic shape is expected for the wave-packet spreading in quantum systems with diffusivelike dynamics.[31,32] Typical asymptotic shapes of the wave packet of two magnons can be visualized in Fig. 6. The initial conditions were chosen to have $d_0 = 2$ (Fig. 6(a)) and $d_0 = N/2$ (Fig. 6(b)). A logarithmic color scale was used to allow for a better analysis of the main trends. In Fig. 6(a) the spin deviations were initially close to the chain center. It shows that the wave-function component with a single deviation displacement over a distance d from the initial position is larger than the component with both spin deviations displaced by a distance $d/2$. This feature is incompatible with a wave packet decomposed as the product of exponentially decaying functions and is more likely to result from a product of power laws. In Fig. 6(b), the spin deviations were far apart (half the chain size). The same above feature is observed with the additional collision effect once two spin deviations are not allowed on the same site.

To quantify the asymptotic form of the wave packet, we measured the probability distribution function associated with a single spin deviation defined as

$$|\phi_{n_1}|^2 = \sum_{n_2} |\phi_{n_1,n_2}|^2, \tag{13}$$

which gives the spatial distribution function of the left-most spin deviation irrespective to the position of the second flipped spin. In order to avoid strong crossovers, i.e., a long short-time transient during which the wave packet does not probe efficiently the underlying disorder, we considered a case of stronger disorder $J_2/J_1 = 5$. In Fig. 7, we plot this

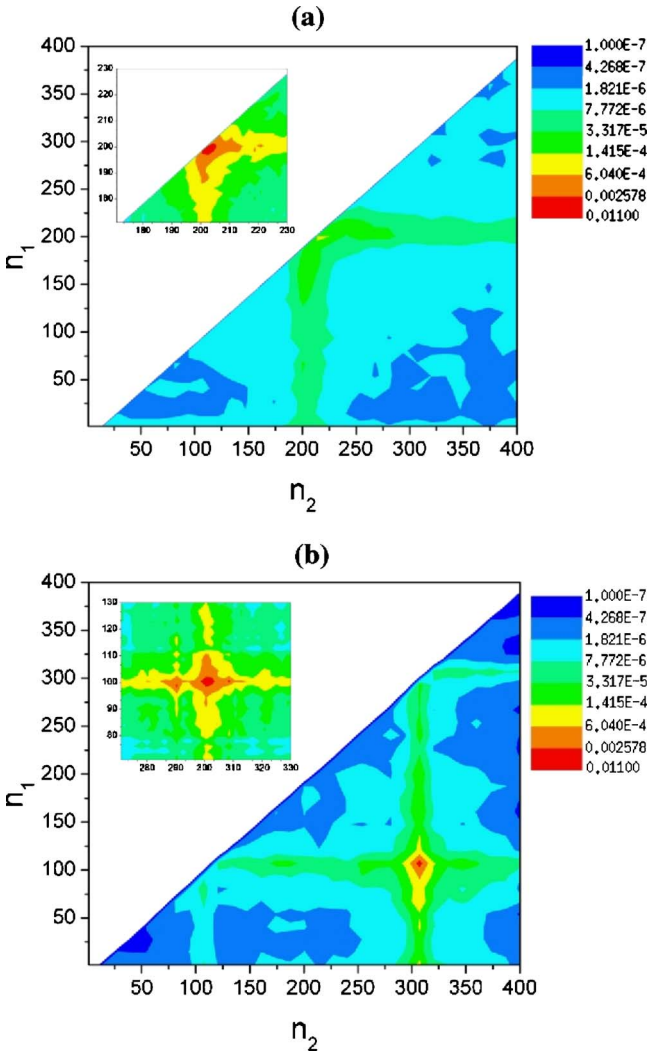

FIG. 6. (Color online) Color representation of the average asymptotic wave-packet probability distribution in logarithmic scale. The initial conditions were chosen to be two spin deviations at a distance (a) $d=2$ and (b) $d=200$ located symmetrically with respect to the chain center. In (b) one notes the collision effect as a result of the exclusion rule.

distribution as obtained after a very long propagation time of a two-spin deviation state with $d_0=2$. One notes that the single-spin wave packet develops power-law tails with distinct characteristic exponents on each side. The larger decay exponent on the right side is a consequence of the effective repulsion between the spins, which make it difficult for the single-spin wave packet to freely spread toward the region predominantly occupied by the second spin excitation.

We further computed the distribution function of the distance between the spin deviations defined as

$$P(d) = \sum_{n_1=1}^{N-d} |\phi_{n_1,n_2=n_1+d}(t)|^2, \tag{14}$$

where the probability amplitudes were taken from a time much larger than the saturation time. The configurational average of the above distribution function is reported in Fig. 8

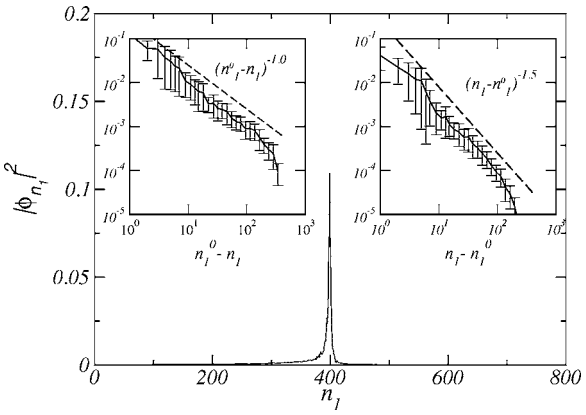

FIG. 7. Asymptotic distribution of the single-spin wave packet in a chain with $N=800$ spins, averaged over 33 realizations. The initial state have spin deviations at sites $n_1=399$ and $n_2=401$. Note that that the wave packet exhibits asymmetric tails. The insets characterize the power-law decay of each tail. The larger decay exponent of the right side of the wave packet reflects the effective repulsion between the spin deviations. Error bars account for fluctuations over distinct disorder realizations.

for the particular case of $d_0=2$. It displays two well-defined regimes. For $d<N/2$, it decays as a power law, with the distribution exponent being given by $P(d)\propto 1/d$. For $d>N/2$, it exhibits a pronounced decay once double-spin deviation displacement are necessary to achieve such distances.

The emergence of distinct power-law exponents governing the single-spin wave packet leads to the possibility that distinct length scales, one related to the distance between the spin deviations and the other related to the lateral spread of the wave packet, may be governed by distinct dynamical exponents. In order to explore this point, we followed the time evolution of the average distance between the flipped spins defined as

$$\langle d(t)\rangle = \sum_{n_1<n_2} (n_2-n_1)|\phi_{n_1,n_2}(t)|^2. \tag{15}$$

In Fig. 9, we show the time evolution of the average distance starting with two spin deviations with $d_0=2$. A configura-

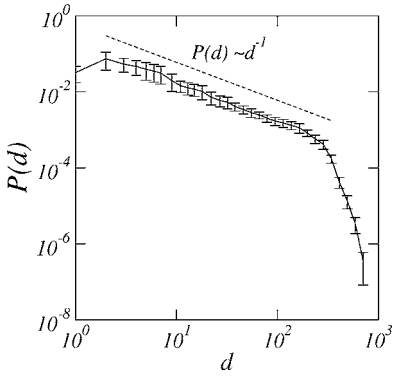

FIG. 8. Asymptotic distribution of the distance between spin deviations in a chain with $N=800$ spins. The regime for $d<N/2$ reflects the power-law decay of the wave-packet envelope. The fast decay for $d>N/2$ is related to the small probability of joint spin-deviation displacements. Error bars account for fluctuations over distinct disorder realizations.

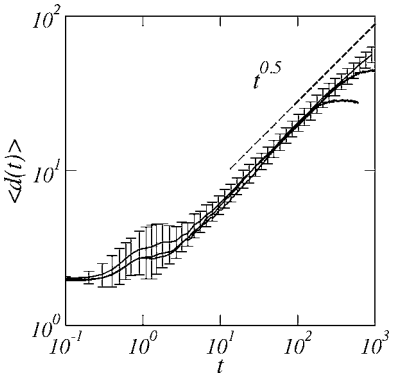

FIG. 9. Time evolution of the average distance between the spin deviations in chains ranging from $N=200$ up 800 spins. The intermediate regime points toward a diffusive separation of the spins with $\langle d(t) \rangle \propto t^{1/2}$. Error bars account for fluctuations over distinct disorder realizations.

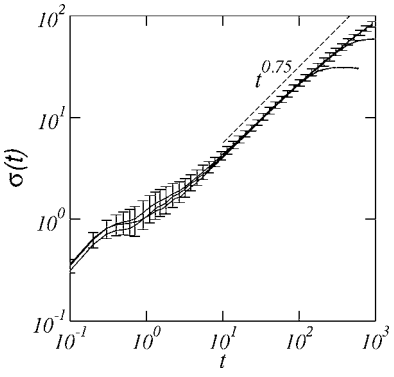

FIG. 10. Time evolution of the average dispersion of the distance between the spin deviations. The intermediate scaling regime is well fitted by a superdiffusive law on the form $\sigma \propto t^{3/4}$. Thus, the wave-packet spread evolves faster than the average spin-spin distance. Error bars account for fluctuations over distinct disorder realizations.

tional average over 33 histories was employed. Results are for the time evolution in chains ranging from $N=200$ up to 800 sites. Note that, after an initial waiting time, the average distance grows diffusively before saturating because of the wave-packet reflection at the chain boundaries. The intermediate interval could be well fitted by a power law with $\langle d(t) \rangle \propto t^{1/2}$. We further measured the distance dispersion $\sigma(t)=\sqrt{\langle d^2(t) \rangle - \langle d(t) \rangle^2}$, where

$$\langle d^2(t) \rangle = \sum_{n_1 < n_2} (n_2 - n_1)^2 |\phi_{n_1,n_2}(t)|^2. \tag{16}$$

The distance dispersion can also be used as a characteristic length scale of the wave-packet spread and starts from $\sigma(0)=0$. Therefore, it is less influenced by the initial transient. Figure 10 shows the dispersion for the same realizations used to compute the average distance. From this, we estimate that the dynamic scaling for the superdiffusive spread is given by $\sigma(t) \propto t^{3/4}$. This exponent is consistent with the superdiffusive spread of single flip excitations.

V. SUMMARY AND CONCLUSIONS

In summary, we investigated some stationary and dynamical aspects of two-magnon excitations in disordered Heisenberg ferromagnetic chains of $S=1/2$ spins. Using a direct numerical diagonalization algorithm, we computed the stationary two-magnon eigenstates on finite chains and characterized their spatial distribution and spin-deviation correlation function. Similarly to the Anderson localization of single-spin collective excitations, the two-magnon states are exponentially localized. The localization length of high-energy states are rather small but diverges as one approaches the ground-state energy. The long localization length of the low-energy states give rises to strong spin-spin correlations that are suppressed at high energies as the localization length becomes smaller than the chain size. One also identified that the distinct roles played by the exclusion rule and the emergence of bound states results in opposite corrections to scaling when referring to the average distance between the spin deviations in finite chains. Furthermore, we followed the time evolution of the distance between two initially localized spin deviations. The asymptotic wave packet develops power-law tails. We computed the asymptotic distribution function of the spin-deviation distance which satisfied $P(d) \propto 1/d$. The single-spin wave packet develops asymmetric tails because of the effective spin-spin repulsion, which give rises to distinct scaling exponents governing the temporal evolution of length scales related to the average spin-spin distance and the wave-packet dispersion. The wave-packet dispersion dynamics is superdiffusive, which is linked to the long localization length of the low-energy states. On the other side, the average distance grows diffusively, indicating that the center of each magnon diffuses independently in the scaling regime.

ACKNOWLEDGMENTS

This work was partially supported by the Brazilian research agencies CNPq and CAPES, as well as by the Alagoas state research agency FAPEAL.

[1] *The Anderson Transition and its Ramifications—Localization, Quantum Interference, and Interactions*, edited by T. Brandes and S. Kettemann (Springer, Berlin, 2003).
[2] P. W. Anderson, Phys. Rev. **109**, 1492 (1958).
[3] E. Abrahams, P. W. Anderson, D. C. Licciardello, and T. V. Ramakrishnan, Phys. Rev. Lett. **42**, 673 (1979). For a review see, e.g., I. M. Lifshitz, S. A. Gredeskul, and L. A. Pastur, *Introduction to the Theory of Disordered Systems* (Wiley, New York, 1988).
[4] T. A. L. Ziman, Phys. Rev. Lett. **49**, 337 (1982).
[5] G. Theodorou, J. Phys. C **15**, L1315 (1982).
[6] R. Riklund and M. Severin, J. Phys. C **21**, L965 (1988).

[7] S. N. Evangelou and D. E. Katsanos, Phys. Lett. A **164**, 456 (1992).
[8] S. N. Evangelou, A. Z. Wang, and S. J. Xiong, J. Phys.: Condens. Matter **6**, 4937 (1994).
[9] F. Domínguez-Adame, V. A. Malyshev, F. A. B. F. de Moura, and M. L. Lyra, Phys. Rev. Lett. **91**, 197402 (2003).
[10] D. L. Shepelyansky, Phys. Rev. Lett. **73**, 2607 (1994).
[11] Y. Imry, Europhys. Lett. **30**, 405 (1995).
[12] K. Frahm, A. Muller-Goeling, J.-L. Pichard, and D. Weinmann, Europhys. Lett. **31**, 169 (1995).
[13] P. Jacquod and D. L. Shepelyansky, Phys. Rev. Lett. **75**, 3501 (1995).
[14] Y. V. Fyodorov and A. D. Mirlin, Phys. Rev. B **52**, R11580 (1995).
[15] K. Frahm, A. Muller-Groeling, and J.-L. Pichard, Phys. Rev. Lett. **76**, 1509 (1996).
[16] M. Leadbeater, R. A. Romer, and M. Schreiber, Eur. Phys. J. B **8**, 643 (1999).
[17] K. Frahm, Eur. Phys. J. B **10**, 371 (1999).
[18] O. Halfpap, Ann. Phys. **10**, 623 (2001).
[19] A. Eilmes, R. A. Romer, and M. Schreiber, Eur. Phys. J. B **23**, 229 (2001).
[20] A. Eilmes, U. Grimm, R. A. Romer, and M. Schreiber, Eur. Phys. J. B **8**, 547 (1999).
[21] R. A. Romer and M. Schreiber, Phys. Rev. Lett. **78**, 515 (1997).
[22] F. J. Dyson, Phys. Rev. **102**, 1217 (1956).
[23] B. W. Southern, T. S. Liu, and D. A. Lavis, Phys. Rev. B **39**, 12160 (1989).
[24] S. R. Aladim and M. J. Martins, J. Phys. A **26**, L529 (1993).
[25] B. W. Southern, J. L. Martinez Cuéllar, and D. A. Lavis, Phys. Rev. B **58**, 9156 (1998).
[26] S. Cojocaru and A. Ceulemans, Europhys. Lett. **61**, 838 (2003).
[27] A. Ceulemans, S. Cojocaru, and L. F. Chibotaru, Eur. Phys. J. B **21**, 511 (2001).
[28] L. F. Santos and M. I. Dykman, Phys. Rev. B **68**, 214410 (2003).
[29] R. D. McMichael, D. J. Twisselmann, and A. Kunz, Phys. Rev. Lett. **90**, 227601 (2003).
[30] O. V. Manko, B. I. Sandovnikov, and A. M. Savchenko, Physica A **343**, 393 (2004).
[31] R. Ketzmerick, K. Kruse, S. Kraut, and T. Geisel, Phys. Rev. Lett. **79**, 1959 (1997).
[32] R. P. A. Lima, F. A. B. F. de Moura, M. L. Lyra, and H. N. Nazareno, Phys. Rev. B **71**, 235112 (2005).